

Probabilistic Wind Power Forecasting with Tree-Based Machine Learning and Weather Ensembles

Max Bruninx¹, Diederik van Binsbergen^{1,2}, Timothy Verstraeten¹, Ann Nowé¹, and Jan Helsen¹

¹Vrije Universiteit Brussel, Brussels, Belgium

²Norwegian University of Science and Technology, Trondheim, Norway

Abstract—Accurate production forecasts are essential to continue facilitating the integration of renewable energy sources into the power grid. This paper illustrates how to obtain probabilistic day-ahead forecasts of wind power generation via gradient boosting trees using an ensemble of weather forecasts. To this end, we perform a comparative analysis across three state-of-the-art probabilistic prediction methods—conformalised quantile regression, natural gradient boosting and conditional diffusion models—all of which can be combined with tree-based machine learning. The methods are validated using four years of data for all wind farms present within the Belgian offshore zone. Additionally, the point forecasts are benchmarked against deterministic engineering methods, using either the power curve or an advanced approach incorporating a calibrated analytical wake model. The experimental results show that the machine learning methods improve the mean absolute error by up to 53% and 33% compared to the power curve and the calibrated wake model. Considering the three probabilistic prediction methods, the conditional diffusion model is found to yield the best overall probabilistic and point estimate of wind power generation. Moreover, the findings suggest that the use of an ensemble of weather forecasts can improve point forecast accuracy by up to 23%.

Keywords— Probabilistic forecasting, gradient boosting trees, offshore wind farms

I. INTRODUCTION

Over the past two decades, the annual growth rate of renewable energy capacity has continued to increase, significantly reducing fossil fuel consumption and global emissions [28]. Nonetheless, the inherent intermittency of renewable energy sources present additional challenges and costs to the power system [23, 56]. Enhancing production forecasts is critical to mitigate these issues and facilitate the continued integration of renewable energy sources into the grid. The importance of this subject is also highlighted by the extensive body of research produced over the past fifty years [26]. Different types of forecasts may be required depending on the application area. For example, day-ahead forecasts can be used to bid on the day-ahead market [42, 22, 12], whereas intra-hour forecasts can help to maintain grid stability [59, 1]. Moreover, these forecasts can take the form of point forecasts, which estimate the conditional mean, or probabilistic forecasts, which aim to capture the entire conditional probability distribution. The widespread recognition in the literature that weather variables

should be modelled as stochastic processes (see, for example, [2, 41]) has shifted the field towards the latter approach [52].

This work studies probabilistic day-ahead forecasting of wind power generation in the context of offshore wind farms. Nonetheless, the presented methodology can also be applied to different renewable energy sources or different forecast horizons. Typically, Numerical Weather Predictions (NWP) are the most important input for day-ahead forecasting and statistical or machine learning models are employed to learn the relationship between the weather forecasts and the power output [18]. The primary advantage of data-driven techniques lies in their ability to adapt wind forecasts to site-specific conditions and mitigate meteorological errors. This is particularly important in the context of day-ahead forecasting, since weather forecasts typically present a high degree of uncertainty at this stage. More specifically, the use of meteorological data introduces two sources of error compared to the true wind conditions on site. First, the weather forecast error, representing the difference between the wind forecasts and the corresponding observations, and second, the location error, which stems from the spatial mismatch between the numerical weather prediction grid and the precise turbine locations. In typical NWP models, grid points are 7-12 km apart, whereas the spacing between offshore wind turbines is around 1 km depending on the rotor size and the lay-out optimization [14]. This is also illustrated in Figure 1 for the Belgian offshore zone. Moreover, the local wind speeds in the wind farm are affected by wake effects [20] and blockage [47], which are not accounted for by the NWP models. In addition to the errors introduced by employing meteorological data, power production can also be influenced by other atmospheric variables besides wind speed, such as turbulence intensity, shear and veer, along with turbine-specific characteristics.

In our work, we will consider tree-based machine learning methods, in particular gradient boosting trees, due to their superior performance in recent wind power forecasting competitions [26, 7, 11]. Moreover, compared to deep learning methods, gradient boosting trees are still found to outperform on tabular data sets [10, 21] and are generally more interpretable. However, tree-based machine learning models produce discrete outputs by default, which means they cannot be directly applied to probabilistic forecasting. To address this

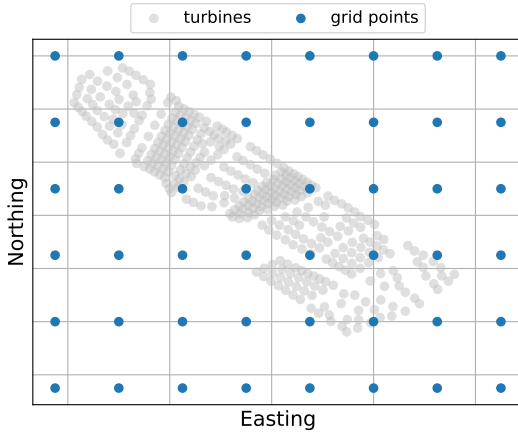


Fig. 1: Location of the turbines in the Belgian offshore zone and the grid points from the DWD ICON-EU model (with a horizontal grid spacing of 6.5 km).

limitation, they can be paired with probabilistic prediction methods that transform their point predictions into predictive distributions. These probabilistic prediction methods can be categorized into parametric methods, which assume an underlying parametric probability distribution, or non-parametric methods, also referred to as distribution-free, which do not make any assumptions on the underlying distribution of the target variable.

Quantile regression [31], a non-parametric method, has emerged as the leading approach for probabilistic forecasting in the field of renewable energy [52]. This method is model-agnostic, as it can be applied to any model that minimises a loss function, such as gradient boosting trees [35]. Conformalized quantile regression [43] extends upon this approach by calibrating the prediction intervals to ensure that they achieve statistically valid coverage. Treeffuser [8], another non-parametric method inspired by recent advances in generative modelling, applies conditional diffusion models on tabular data using gradient boosting trees. This method produces probabilistic forecasts by drawing samples from the conditional distribution learned by the model. Empirically, Treeffuser was found to achieve superior performance for probabilistic and point forecasting on a wide range of publicly available data sets from other fields. In terms of parametric methods, natural gradient boosting [17] and probabilistic gradient boosting machines [50] are the most well-known in the area of tree-based machine learning. Whereas the former can estimate the parameters of any probability distribution, the latter is limited to distributions for which the parameters can be expressed in terms of mean and variance.

This study aims to assess which probabilistic prediction methods are the most suitable in the context of wind power forecasting. For this purpose, we consider three state-of-the-art methods, namely conformalised quantile regression, natural gradient boosting and conditional diffusion models. The main contributions of the article are the following:

- We demonstrate how these three methods can be combined with gradient boosting trees to generate probabilistic forecasts of wind power production. Although the first two methods have been applied in prior research on wind power forecasting [27, 55, 58, 33], this study is the first to directly compare them and to include the third approach, namely conditional diffusion models via gradient boosting trees.
- We provide an extensive validation of the different methods, considering four years of data and encompassing all wind farms within the Belgian offshore zone. This contrasts with existing literature, which often relies on data sets restricted to one or two wind farms and shorter time horizons. Furthermore, we also consider an ensemble of weather forecasts rather than a single weather forecast and showcase how this improves predictive performance.
- We benchmark the methods against deterministic engineering approaches, employing a well-established method using the power curve and an advanced approach based on a calibrated analytical wake model. This direct comparison against engineering methods is often overlooked in existing studies using machine learning.

The remainder of the paper is organised as follows: Section II provides an overview of the forecasting methodology, covering the different methods as well as the use of an ensemble of weather forecasts. Section III details the experiments conducted across all wind farms within the Belgian offshore zone, while Section IV covers the experimental outcomes. Finally, Section V concludes the work.

Note: Throughout the paper, symbols with a hat ($\hat{\cdot}$) denote model predictions and bold symbols indicate vectors. For an observation i , the target variable is given by y_i and the feature vector by \mathbf{x}_i . $F_i(\cdot)$ is the cumulative density function and $q_{i,\tau}$ or $F_i^{-1}(\tau)$ are used interchangeably for the τ -quantile prediction. Last, the significance level $\alpha \in [0, 1]$, determines the $(1 - \alpha)\%$ confidence interval \mathcal{C}_α .

II. METHODOLOGY

In Figure 2, an overview of the probabilistic day-ahead forecasting methodology is presented. The method aims to model the conditional power distribution given an ensemble of different weather forecasts. To this end, gradient boosting trees are combined with three state-of-the-art probabilistic predictions methods: conformalised quantile regression, natural gradient boosting and conditional diffusion models. Section II-A discusses the different weather forecasts and how they are preprocessed. Sections II-B to II-D cover the details of the different probabilistic predictions methods. Last, Section II-E explains the deterministic benchmark models used to evaluate point forecast performance.

A. Weather forecasts

Following the typical model chain, the day-ahead wind speed and wind direction forecasts are used as input to the models [18]. Instead of relying on one weather forecast provider, we combine forecasts from different providers to

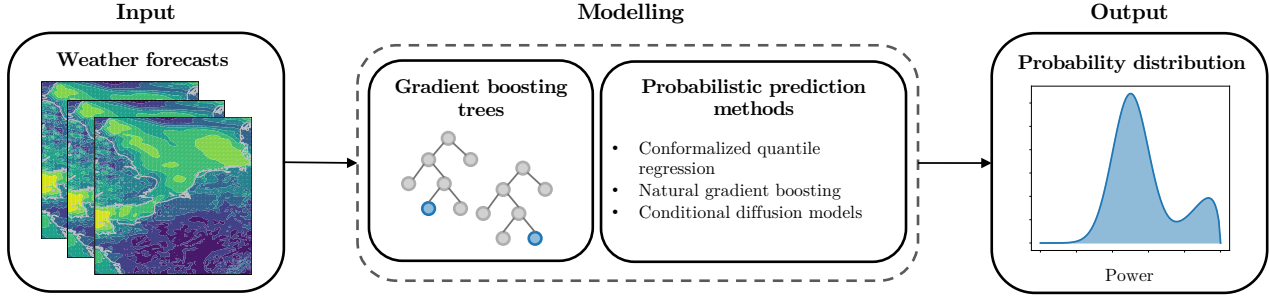


Fig. 2: High-level overview of the probabilistic forecasting methodology.

incorporate the uncertainty between these forecasts. For simplicity, we only considered the weather forecasts related to one specific grid point, namely the closest point to the center of the Belgian offshore zone. However, empirical results suggested that considering multiple grid points could improve forecasting models [4] and, therefore, it is an interesting addition for future research.

The forecasts are further processed by including lagged variables, i.e., the forecasts of the previous and the next hours, similar to the approach in [3]. Furthermore, summary statistics for each hour are calculated such as the mean and the standard deviation. Note that for the wind direction it is important to consider the circular mean and standard deviation [34].

B. Conformalized quantile regression

Conformalized quantile regression [43] combines classical quantile regression with conformal prediction. This method allows to construct distribution-free probability estimates with a statistical coverage guarantee.

In a quantile regression model [31], the quantile loss

$$L(y_i, \hat{q}_{i,\tau}) = \begin{cases} \tau (y_i - \hat{q}_{i,\tau}) & y_i \geq \hat{q}_{i,\tau} \\ (1 - \tau) (\hat{q}_{i,\tau} - y_i) & y_i < \hat{q}_{i,\tau} \end{cases}, \quad (1)$$

is used to directly estimate the τ -quantile $q_{i,\tau}$ rather than the target variable. This method is flexible, in the sense that it can be applied to any model that minimises a loss function, and distribution-free, meaning that it does not make any assumption on the underlying distribution of the target variable. However, this method does not guarantee valid coverage of the intervals defined by the quantile predictions.

Conformal prediction is a calibration procedure which can be used to attain a statistically guaranteed marginal coverage for any prediction set:

$$1 - \alpha \leq \mathbb{P}(y_i \in \mathcal{C}^{\text{CP}}(\mathbf{x}_i)) \leq 1 - \alpha + \frac{1}{n+1}, \quad (2)$$

with (\mathbf{x}_i, y_i) an unseen observation from the same data distribution as the calibration set, $\mathcal{C}^{\text{CP}}(\mathbf{x}_i)$ the prediction set after calibration and n the number of samples in the calibration set. To this end, the conformal score is first computed for each observation in a hold-out calibration set. Afterwards, the $\frac{(n+1)(1-\alpha)}{n}$ empirical quantile of this score is used to adapt the prediction set. The conformal score quantifies how the

observed value differs from the model output and is also referred to as a nonconformity measure. An overview of conformal scores in a regression setting can be found in [30]. We also refer the reader to [5] for an introduction to conformal prediction.

In the context of conformalized quantile regression, the conformal score for the confidence interval obtained by quantile regression

$$\mathcal{C}_\alpha(\mathbf{x}_i) = [\hat{q}_{i,\alpha/2}, \hat{q}_{i,1-\alpha/2}], \quad (3)$$

is given by:

$$s(\mathbf{x}_i, y_i) = \max \{ \hat{q}_{i,\alpha/2} - y_i, y_i - \hat{q}_{i,1-\alpha/2} \}. \quad (4)$$

The score is positive when the observed value lies outside of the prediction interval and increases when the distance towards the prediction interval increases. After computing the empirical quantile of the conformal scores on the calibration set \hat{s} , the confidence interval is adapted accordingly:

$$\mathcal{C}_\alpha^{\text{CP}}(\mathbf{x}_i) = [\hat{q}_{i,\alpha/2} - \hat{s}, \hat{q}_{i,1-\alpha/2} + \hat{s}]. \quad (5)$$

This is also illustrated visually in Figure 3.

Note that quantile regression does not guarantee that the predicted quantiles are non-crossing, i.e., that lower-level quantiles are always lower or equal to higher-level quantiles. To resolve this issue, we employ the post-processing technique presented in [13], where the quantile predictions are sorted to enforce monotonicity.

C. Natural gradient boosting

Natural gradient boosting [17] is a parametric probabilistic prediction method that leverages gradient boosting trees. Unlike traditional gradient boosting regression, which estimates the target variable, the model estimates the parameters of a conditional probability distribution given the input variables. In this work, we will assume a Normal or Gaussian distribution, with the cumulative density function given by:

$$F(y; \mu, \sigma) = \frac{1}{\sigma\sqrt{2\pi}} \int_{-\infty}^y \exp\left(-\frac{(t-\mu)^2}{2\sigma^2}\right) dt. \quad (6)$$

The conditional parameters μ_i and σ_i are estimated by optimising the scoring rule through gradient descent, for which we consider the logarithmic score:

$$\mathcal{L}(y_i, \hat{\theta}_i) = -\log P_{\hat{\theta}_i}(y_i), \quad (7)$$

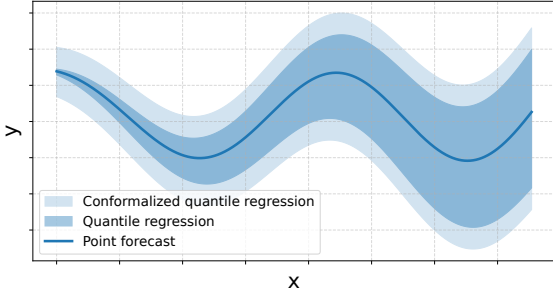


Fig. 3: Visual example of the conformal prediction procedure with conformalized quantile regression from (5), with the empirical quantile of the conformal scores $\hat{s} > 0$. The dark blue area indicates the confidence interval predicted by the quantile regression model and the light blue area shows how the confidence interval is adapted after conformal calibration. The difference between the light blue and the dark blue area is determined by the empirical quantile of the conformal scores \hat{s} .

with $\hat{\theta}_i = \{\hat{\mu}_i, \hat{\sigma}_i\}$ and P_θ the likelihood function. To improve the learning dynamics, the model employs the natural gradient rather than the (ordinary) gradient for gradient descent.

D. Conditional diffusion models

Treeffuser [8] is a score-based conditional diffusion model for tabular data via gradient boosting machines. In score-based diffusion models [49], the forward diffusion process maps the data distribution p_0 to a noise distribution p_T using a stochastic differential equation:

$$d\mathbf{y} = f(\mathbf{y}, t)dt + g(t)d\mathbf{w}, \quad (8)$$

with $\mathbf{w}(t)$ a standard Brownian motion, f the drift function and g the diffusion function. The reverse diffusion process, that can be used to generate samples from p_0 using p_t , is then given by:

$$d\mathbf{y} = [f(\mathbf{y}, t) - g^2(t)\nabla_{\mathbf{y}} \log p_t(\mathbf{y})] dt + g(t)d\tilde{\mathbf{w}}, \quad (9)$$

where $\tilde{\mathbf{w}}$ is a standard Brownian motion with reverse time and $\nabla_{\mathbf{y}} \log p_t(\mathbf{y})$ represent the score function, which is unknown and should be estimated from data by a model. Conditional diffusion models aim to construct a diffusion model conditional on some input variables. This can either be attained by post-processing the output of a diffusion model using guidance methods [16, 25] or incorporating the information in the training step [6, 44]. Treeffuser employs the latter approach.

Conditional diffusion models can provide probabilistic predictions by sampling from the conditional distribution and computing the empirical quantiles from these samples. In this work, we draw 50 samples to calculate these empirical quantiles.

E. Deterministic benchmark models

The simplest way to obtain a deterministic power forecasts, which is often used in practice, is to apply the wind speed

forecast to the power curve of the manufacturer for each turbine present in the wind farm:

$$\hat{y}_i = \sum_{j=1}^m P_j^M(v_{i,s}), \quad (10)$$

with m the number of turbines in the farm, $P_j^M(\cdot)$ the manufacturer power curve of turbine j and $v_{i,s}$ the wind speed forecast.

However, this method does not consider the wake effect present in wind farms, where upstream wind turbines affect the available wind energy of downstream turbines, resulting in reduced power production [20]. Consequently, power forecasts produced using this method will overestimate the actual possible power production.

To account for wake effects, analytical wake models are commonly used. These steady-state models account for intra-farm and inter-farm wake effects by considering, respectively, the layout of the target wind farm as well as the neighbouring wind farms. To this end, the self-similar Gaussian wake model of Niayifar & Porté-Agel [37] as implemented in the PyWake framework [40] is employed, where the deterministic power forecast is calculated as follows:

$$\hat{y}_i = \sum_{j=1}^m P_j^W(v_{i,s}, v_{i,d}), \quad (11)$$

with m being the number of turbines in the farm, $P_j^W(\cdot)$ the power production of turbine j calculated using the power curve and the local wind speed acquired from the analytical wake model, and $v_{i,s}$, $v_{i,d}$ are the wind speed and wind direction forecast, respectively.

The recovery rate of the wake in the model depends on two parameters: one that varies with the local turbulence intensity, and one that remains constant. These two parameters are calibrated for the Belgian-Dutch offshore cluster using SCADA data from multiple wind farms, following the procedure described in [53] and applied in [9, 54]. The local turbulence intensity is obtained by combining the freestream turbulence intensity, which is calculated according to the IEC standard [57], and the wake-added turbulence intensity, resulting from the Crespo-Hernández model [15]. The velocity deficit due to wake overlap is calculated using linear superposition [29], consistent with [37].

III. EXPERIMENTS

A. Set-up

We evaluate the models on all wind farms present in the Belgian offshore zone, as visualized in Figure 4. To this end, we gather a dataset with data ranging from 2021 to 2024 with a resolution of one hour. The first three years are used to train the models, whereas the last year is used to evaluate the models. When a validation or calibration set is required, the data of 2023 is held-out from the training set.

The hyperparameters of each model were optimized using random search with 25 iterations, the search space of the

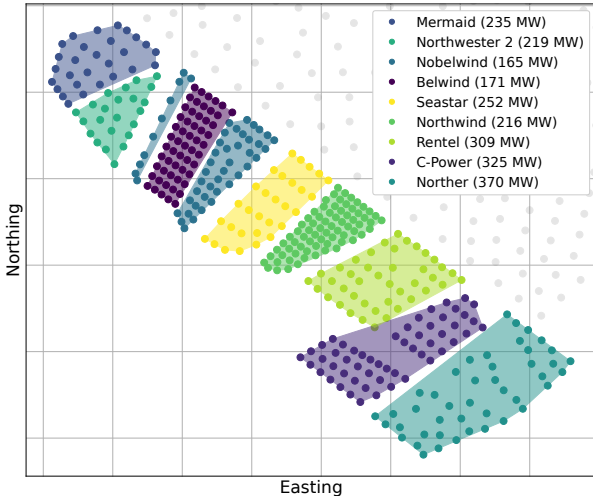


Fig. 4: The wind farms present in the Belgian offshore zone (in color) and the surrounding wind turbines from Borssele wind farm zone (NL) (in grey). In total, the Belgian offshore zone comprises more than 2 GW of installed capacity divided over 9 different wind farms. The first project, C-Power, was built in 2009 and the last projects, Mermaid and Northwester 2, were finished in 2020. The Borssele wind farm zone is operational since 2021.

hyperparameters can be found in A. For the Treeffuser model, we also include a model with the default hyperparameters since the authors suggested that hyperparameter tuning is not required [8].

The models used in the experiments are referred to as follows: Power curve (10), Wake model (11), CQR (Section II-B), NGBoost (Gaussian) (Section II-C), and Treeffuser along with its variant without hyperparameter tuning, Treeffuser (no tuning) (Section II-D). The first two models are deterministic models based on engineering methods, which we use as a baseline, whereas the other models are probabilistic forecasting models. Note that the engineering methods do not account for grid losses present in the data set. Therefore, their predictions are re-scaled using the ratio of the maximum observed power over the rated power.

B. Data

Generation data at grid connection is obtained from the ENTSO-E Transparency Platform [39]. To remove large curtailments from the data set, observations for which downward balancing bids were activated for any wind farm in the Belgian offshore zone are filtered out based on data provided by Elia [45]. We explicitly filter out these observations since they would result in forecasts that underestimate possible power generation. Unfortunately, the available data does not allow to filter out curtailments ordered by the Balance Responsible Party of the wind farm. As a proxy for these economic curtailments, we use ERA-5 reanalysis data to group observations into wind speed bins and remove any observation from the training set with a power below the 5th percentile of its bin.

The bin size is set to 0.5 m/s, in accordance with the IEC standard [57], except when a bin contains fewer than 100 observations, in which case the bin size is incremented by 0.5 m/s until the bin contains sufficient observations.

The analysis incorporates five day-ahead weather forecasts, including the Deutscher Wetterdienst's ICON-EU and ICON-D2 models, as well as forecasts from the ECMWF HRES, Météo France ARPEGE-EU, and Met Office Global Hi-Res models. These forecasts were obtained from a commercial weather forecast provider. The weather forecasts are pre-processed as described in Section II-A. For the engineering models, the average day-ahead wind speed and direction forecasts over the different providers are used as input.

C. Performance metrics

The models are evaluated on their point forecast and probability estimate. When evaluating the probability estimates, the 5th, 10th, 25th, 50th, 75th, 90th, and 95th percentiles of the conditional distribution are considered to ensure comparability between the methods. We define the point forecast of the models as the median prediction. The evaluation metrics are normalised by the installed capacity of the farm. On average the installed capacity per wind farm in the Belgian offshore zone is around 250 MW, implying that a relative forecast error of 1% represents an absolute error of around 2.5 MW.

The Mean Absolute Error (MAE) is used to evaluate the point forecasts of the models:

$$MAE = \frac{1}{n} \sum_{i=1}^n |y_i - \hat{y}_i|, \quad (12)$$

where n equals the number of samples in the evaluation set.

Probability estimates are evaluated using the Continuous Rank Probability Score (CRPS) [36, 24]:

$$CRPS = \int_{-\infty}^{+\infty} \left(\hat{F}_i(t) - \mathbb{1}(y_i \leq t) \right)^2 dt, \quad (13)$$

with $\mathbb{1}$ the indicator function. This metric is then averaged over all observations. CRPS is a proper scoring rule, which measures reliability, i.e., how well the forecast probabilities align with the observed frequencies of events, and sharpness, i.e., how concentrated the probabilistic forecasts are around the actual outcomes [24, 19]. Another interesting property is that for a point forecast the CRPS equals the MAE. Given that not all forecasting methods predict the entire cumulative density function, we employ the formulation proposed by [38]:

$$CRPS = \int_0^1 L(y_i, \hat{q}_{i,\tau}) d\tau, \quad (14)$$

where $L(\cdot)$ equals the quantile loss (1). For a discrete set of quantile predictions, the CRPS can be approximated by a Riemann sum.

IV. RESULTS AND DISCUSSION

Table I shows the mean absolute error of the different models on the test set. The Treeffuser model with parameter tuning is found to consistently achieve the best performance

TABLE I: Out-of-sample normalised mean absolute error per wind farm, as well as the average score over the wind farms. The metric is normalised by the installed capacity of the wind farm. Lower scores indicate a better fit, with the best scores highlighted in bold.

	Power curve	Wake model	NGBoost (Gaussian)	CQR	Treeffuser (no tuning)	Treeffuser
Belwind	15.6%	10.5%	7.5%	7.2%	7.1%	7.0%
C-Power	15.3%	10.8%	7.7%	7.3%	7.1%	7.0%
Mermaid	14.5%	12.2%	9.2%	9.0%	9.2%	9.0%
Nobelwind	17.6%	12.2%	8.4%	8.3%	8.2%	8.1%
Norther	14.3%	10.9%	8.5%	8.2%	8.1%	7.9%
Northwester 2	20.7%	15.2%	9.3%	8.9%	8.9%	8.9%
Northwind	21.1%	11.8%	8.2%	7.9%	7.7%	7.6%
Rentel	16.8%	11.8%	8.8%	8.7%	8.7%	8.5%
Seastar	15.8%	11.9%	8.8%	8.5%	8.4%	8.4%
Average	16.9%	11.9%	8.5%	8.2%	8.2%	8.0%

TABLE II: Normalised continuous rank probability score per wind farm, as well as the average score over all wind farms. The values between brackets indicate the normalised CRPS on the training data. The metric is normalised by the installed capacity of the wind farm. Lower scores indicate a better fit, with the best scores highlighted in bold.

	NGBoost (Gaussian)	CQR	Treeffuser (no tuning)	Treeffuser
Belwind	5.2% (4.6%)	5.0% (4.7%)	5.2% (1.6%)	4.8% (4.1%)
C-Power	5.4% (4.6%)	5.0% (4.1%)	5.2% (1.6%)	4.9% (3.5%)
Mermaid	6.5% (5.4%)	6.3% (5.3%)	6.8% (1.9%)	6.2% (4.8%)
Nobelwind	6.0% (5.3%)	5.7% (5.1%)	6.0% (1.9%)	5.6% (4.6%)
Norther	6.1% (5.1%)	5.8% (5.0%)	5.9% (1.8%)	5.6% (3.6%)
Northwester 2	6.5% (5.1%)	6.1% (5.0%)	6.6% (2.0%)	6.1% (5.2%)
Northwind	5.7% (5.2%)	5.4% (4.7%)	5.6% (1.7%)	5.2% (4.4%)
Rentel	6.3% (4.8%)	6.1% (4.6%)	6.5% (1.7%)	6.0% (4.4%)
Seastar	6.1% (5.3%)	5.8% (5.1%)	6.2% (2.0%)	5.8% (5.2%)
Average	6.0% (5.0%)	5.7% (4.8%)	6.0% (1.8%)	5.6% (4.4%)

for all wind farms, with an improvement in MAE of 53% compared to the power curve. Between the probabilistic forecasting models, the natural gradient boosting model (with a Normal distribution) achieves the worst performance. This is an interesting result because it suggests that even the point forecasts are affected by the probabilistic forecasting technique. We also note the analytical wake model improves MAE by 30% compared to the power curve, indicating the importance of accurately modelling wake effects. Due to this significant difference in predictive performance, results derived from the power curve method will not be further discussed in the remainder of this paper. When comparing the probabilistic forecasting models against the analytical wake model, we find an additional improvement in average MAE of up to 33%. The improved performance may be explained by the fact that the machine learning model can also account for the weather forecast error, whereas the wake model treats the wind speed and direction forecast as an exact input. In addition, we note that the potential gains in MAE fluctuate between the different wind farms. These fluctuations could be attributed to the fundamental difference between analytical wake models

and machine learning methods. While the former explicitly models the wake effects within the farm, the latter implicitly accounts for all patterns in the data affecting the power output. Therefore, machine learning methods can also consider external factors such as active curtailment strategies, which may be present in the operational context of certain wind farms. When the forecasts should estimate the potential power generation rather than the actual production, analytical wake models provide an alternative to filtering out observations with curtailments from the data set.

In Table II, the normalised continuous rank probability scores on the train and test set are shown for all wind farms. Consistent with the results in Table I, the Treeffuser model with optimized hyperparameters achieves the best out-of-sample performance. By contrast, and in opposition to the observations of [8], our findings indicate that the Treeffuser model without hyperparameter tuning ranks among the lowest performers. This can be attributed to overfitting, as we find that the model obtains significantly better performance on the train set compared to the test set. For this reason, we do not consider this model in the remainder of the paper. We also note that

TABLE III: Evaluation metrics per operating region of the power curve averaged over the different wind farms. Normalisation is done using the installed capacity of the farm. Lower scores indicate a better fit, with the best scores highlighted in bold.

(a) Normalised mean absolute error

	Wake model	Treeffuser	CQR	NGBoost (Gaussian)
Region 1	0.8%	0.6%	0.8%	1.7%
Region 2	13.3%	8.9%	9.0%	9.2%
Region 3	11.5%	8.2%	8.6%	8.8%

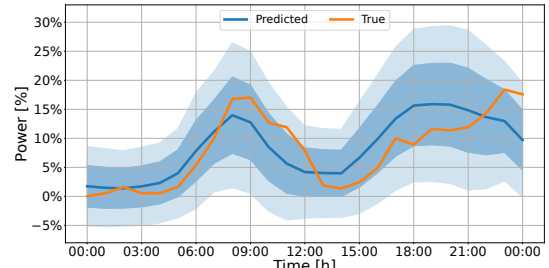
(b) Normalised continuous ranked probability score

	Wake model	Treeffuser	CQR	NGBoost (Gaussian)
Region 1	NA	0.6%	0.7%	1.4%
Region 2	NA	6.1%	6.2%	6.4%
Region 3	NA	5.9%	6.1%	6.5%

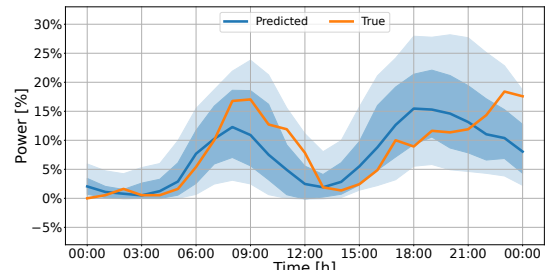
the natural gradient boosting model is again amongst the worst performers, which could indicate that the Normal distribution is not a good fit to model the conditional power distribution.

Table III shows the average score across the wind farms per operating region of the power curve. The operating region is determined based on the average wind speed forecast. Traditionally, four different operating regions are defined based on the wind speed [46]: The first region covers wind speeds below the cut-in speed. The second region includes all wind speeds between the cut-in and rated wind speeds. The third region is defined by wind speeds ranging from the rated wind speed to the cut-out wind speed. The final region encompasses all wind speeds above the cut-out wind speed. However region four is excluded from the analysis due to a lack of sufficient observations. This region is also strongly associated with storm events and cut-out events, which are known to cause the largest errors in day-ahead wind power forecasts [51]. Consequently, specialized storm forecasting tools, such as [48], are often employed for these conditions. The largest discrepancy between the performance of the natural gradient boosting model and the other probabilistic forecasting models is in operating regions 1 and 3. This supports our belief that the Normal distribution is not a good fit to model the conditional power distribution, since in these operating regions the power output is not symmetrically distributed [32]. The two other methods are distribution-free, meaning that they do not assume an underlying parametric distribution, and therefore they can provide probability distribution of any shape. This difference is also illustrated in Figure 5, where the predictions of the different probabilistic forecasting models are visualized for a day where the wind speed forecast was around the cut-in wind speed. The confidence interval of the natural gradient boosting model contains negative power outputs, which is not realistic, whereas for the other two methods this issue does not occur.

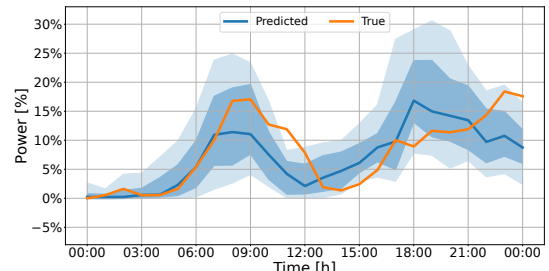
In Figure 6, we illustrate how the use of an ensemble of weather forecasts impacts the MAE of the forecasting models. To this end, we trained the Treeffuser model with



(a) Natural gradient boosting



(b) Conformalized quantile regression



(c) Conditional diffusion model (Treeffuser)

Fig. 5: Illustrative example of the different day-ahead forecasts (including 50% and 80% confidence intervals) where the wind speed forecast was around the cut-in wind speed during the day.

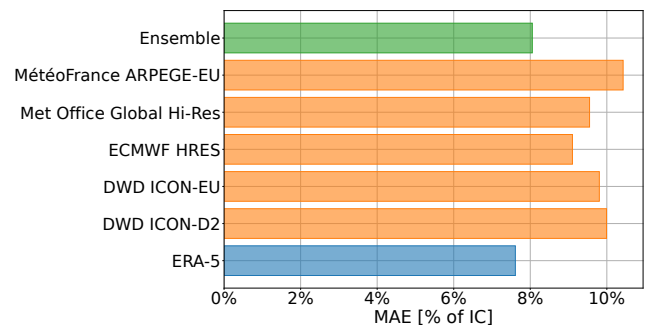


Fig. 6: Average mean absolute error (as a % of the installed capacity of the wind farm) for the Treeffuser model over the different wind farms with different input data sets: ensemble of weather forecasts (green), single weather forecast (orange), re-analysis weather data (blue).

different input data sets: the ensemble of weather forecasts, the individual forecasts and ERA-5 reanalysis data. The reanalysis

data are used to assess the impact of the weather forecast error, as they are derived using data assimilation by combining actual wind speed and direction observations with a weather model. For each input data set, the model was trained on the data of all different wind farms and the average MAE was taken over all wind farms. The results demonstrate that the ensemble model substantially improves predictive performance relative to the individual forecasts, even attaining an MAE close to the value obtained using the reanalysis wind speed and direction from ERA-5. Compared to the worst-performing model, which is the one based on data of MétéoFrance, the ensemble method achieves an improvement of 23%. This observation also supports our belief that the machine learning models could potentially reduce the day-ahead weather forecast error.

In summary, the empirical results indicate that machine learning methods outperform engineering methods for day-ahead forecasting of wind power. These methods can achieve an improved point forecast accuracy of up to 33% and 53% compared to the power curve and the analytical wake model, while also providing an estimate of the predictive distribution. Furthermore, the findings suggest that incorporating an ensemble of weather forecasts significantly enhances predictive accuracy relative to using a single forecast. This represents another advantage compared to engineering methods, which presume the wind speed and direction to be known, and cannot handle multiple weather inputs. Nonetheless, the analytical wake model already shows a considerable improvement compared to the power curve and can be a good alternative to machine learning methods when interpretability is more important and probabilistic estimates are not required. Moreover, the analytical wake models can provide an unbiased estimation of potential power generation when the wind farm pursues an active curtailment strategy. Between the different probabilistic prediction methods, we find that conditional diffusion model consistently attains the best overall point and probabilistic estimate of wind power generation across all wind farms. On the other hand, we observed a significantly higher computation time for training and inference while using this method in our experiments. Conformalized quantile regression obtained a comparable performance at lower computation time and can therefore provide a valuable alternative to conditional diffusion. The natural gradient boosting model achieves the worst performance, especially when the forecasted wind speed is below the cut-in or above the rated wind speed. However, in our work, this method assumes a Normal distribution, which is not a good fit to model wind power uncertainty around cut-in wind speeds. An interesting pursuit for future research could be to extend the methodology to other parametric distributions, such as a mixture of univariate Gaussian densities or a Beta distribution.

V. CONCLUSION

This work studied three different methods for probabilistic day-ahead forecasting of wind power generation using tree-based machine learning and an ensemble of weather forecasts. To this end, we conducted a comparative analysis using data

from all wind farms within the Belgian offshore zone over a period of four years. Alongside the machine learning methods, we also considered deterministic engineering methods, using either the power curve or an analytical wake model.

Our findings showed that the machine learning methods are more accurate compared to the engineering methods, with the conditional diffusion model yielding the most accurate probabilistic and point estimates of wind power generation. Another advantage of the machine learning methods is their ability to incorporate an ensemble of weather forecasts, which can considerably improve predictive performance. Nonetheless, we found that analytical wake models present a good alternative to machine learning methods when interpretability is more important and probabilistic forecasts are not required.

ACKNOWLEDGMENTS

The authors gratefully acknowledge the financial support of the Flemish Government through the Flanders AI Research Program, the Energy Transition Funds of the Belgian Federal Government through the BeFORECAST project and the Sustainable Blue Economy Partnership through the INSPIRE project (project no. SBEP2023-440).

REFERENCES

- [1] Mehrnaz Ahmadi, Hamed Aly, and Mehdi Khashei. 2025. Enhancing Power Grid Stability with a Hybrid Framework for Wind Power Forecasting: Integrating Kalman Filtering, Deep Residual Learning, and Bidirectional LSTM. *Energy*, 137752, 137752.
- [2] Myles R Allen and David A Stainforth. 2002. Towards objective probabilistic climate forecasting. *Nature*, 419, 6903, 228–228.
- [3] Stijn Ally, Timothy Verstraeten, Pieter-Jan Daems, Ann Nowé, and Jan Helsen. 2025. Modular deep learning approach for wind farm power forecasting and wake loss prediction. *Wind Energy Science*, 10, 4, 779–812.
- [4] José R Andrade and Ricardo J Bessa. 2017. Improving renewable energy forecasting with a grid of numerical weather predictions. *IEEE Transactions on Sustainable Energy*, 8, 4, 1571–1580.
- [5] Anastasios N Angelopoulos and Stephen Bates. 2021. A gentle introduction to conformal prediction and distribution-free uncertainty quantification. *arXiv preprint arXiv:2107.07511*.
- [6] Georgios Batzolos, Jan Stanezuk, Carola-Bibiane Schönlieb, and Christian Etmann. 2021. Conditional image generation with score-based diffusion models. *arXiv preprint arXiv:2111.13606*.
- [7] Kevin Bellinguer, Valentin Mahler, Simon Camal, and Georges Karinotakis. 2020. Probabilistic forecasting of regional wind power generation for the eem20 competition: a physics-oriented machine learning approach. In *2020 17th International Conference on the European Energy Market (EEM)*. IEEE, 1–6.
- [8] Nicolas Beltran Velez, Alessandro A Grande, Achille Nazaret, Alp Kucukelbir, and David Blei. 2024. Trefffuser: probabilistic prediction via conditional diffusions with gradient-boosted trees. *Advances in Neural Information Processing Systems*, 37, 118296–118325.
- [9] Diederik van Binsbergen, Pieter-Jan Daems, Timothy Verstraeten, Amir Nejad, and Jan Helsen. 2024. Scalable scada-based calibration for analytical wake models across an offshore cluster. *Journal of Physics: Conference Series*, 2745, 1, (Apr. 2024), 012014. doi:[10.1088/1742-6596/2745/1/012014](https://doi.org/10.1088/1742-6596/2745/1/012014).
- [10] Vadim Borisov, Tobias Leemann, Kathrin Seßler, Johannes Haug, Martin Pawelczyk, and Gjergji Kasneci. 2022. Deep neural networks and tabular data: a survey. *IEEE transactions on neural networks and learning systems*, 35, 6, 7499–7519.
- [11] Jethro Browell, Sebastian Haglund, Henrik Kälvegren, Edoardo Simioni, Ricardo Bessa, Yi Wang, and Dennis van der Meer. 2023. Hybrid energy forecasting and trading competition. (2023). doi:[10.21227/5hn-0891](https://doi.org/10.21227/5hn-0891).

[12] Max Bruninx, Timothy Verstraeten, Jalal Kazempour, and Jan Helsen. 2025. Day-ahead bidding strategies for wind farm operators under a one-price balancing scheme. In *Proceedings of the 16th ACM International Conference on Future and Sustainable Energy Systems*, 719–726.

[13] Victor Chernozhukov, Iván Fernández-Val, and Alfred Galichon. 2010. Quantile and probability curves without crossing. *Econometrica*, 78, 3, 1093–1125.

[14] Thomas C Corke and Robert C Nelson. 2018. *Wind energy design*. CRC Press.

[15] A. Crespo and J. Hernandez. 1996. Turbulence characteristics in wind-turbine wakes. *Journal of Wind Engineering and Industrial Aerodynamics*, 61, 1, (June 1996), 71–85. doi:[10.1016/0167-6105\(95\)00033-x](https://doi.org/10.1016/0167-6105(95)00033-x).

[16] Prafulla Dhariwal and Alexander Nichol. 2021. Diffusion models beat GANs on image synthesis. *Advances in neural information processing systems*, 34, 8780–8794.

[17] Tony Duan, Avati Anand, Daisy Yi Ding, Khanh K Thai, Sanjay Basu, Andrew Ng, and Alejandro Schuler. 2020. Ngboost: natural gradient boosting for probabilistic prediction. In *International conference on machine learning*. PMLR, 2690–2700.

[18] Gregor Giebel and George Kariniotakis. 2017. Wind power forecasting—a review of the state of the art. *Renewable energy forecasting*, 59–109.

[19] Tilman Gneiting, Fadoua Balabdaoui, and Adrian E Raftery. 2007. Probabilistic forecasts, calibration and sharpness. *Journal of the Royal Statistical Society Series B: Statistical Methodology*, 69, 2, 243–268.

[20] Francisco González-Longatt, Peter Wall, and Vladimir Terzija. 2012. Wake effect in wind farm performance: steady-state and dynamic behavior. *Renewable Energy*, 39, 1, 329–338.

[21] Léo Grinsztajn, Edouard Oyallon, and Gaël Varoquaux. 2022. Why do tree-based models still outperform deep learning on typical tabular data? *Advances in neural information processing systems*, 35, 507–520.

[22] Yannick Heiser, Farzaneh Pourahmadi, and Jalal Kazempour. 2025. Betting vs. trading: learning a linear decision policy for selling wind power and hydrogen. *Sustainable Energy, Grids and Networks*, 101848.

[23] Philip J Heptonstall and Robert JK Gross. 2021. A systematic review of the costs and impacts of integrating variable renewables into power grids. *Nature Energy*, 6, 1, 72–83.

[24] Hans Hersbach. 2000. Decomposition of the continuous ranked probability score for ensemble prediction systems. *Weather and Forecasting*, 15, 5, 559–570.

[25] Jonathan Ho and Tim Salimans. 2022. Classifier-free diffusion guidance. *arXiv preprint arXiv:2207.12598*.

[26] Tao Hong, Pierre Pinson, Shu Fan, Hamidreza Zareipour, Alberto Troccoli, and Rob J. Hyndman. 2016. Probabilistic energy forecasting: global energy forecasting competition 2014 and beyond. *International Journal of Forecasting*, 32, 3, 896–913. doi:<https://doi.org/10.1016/j.ijforecast.2016.02.001>.

[27] Jiaming Hu, Qingxi Luo, Jingwei Tang, Jiani Heng, and Yuwen Deng. 2022. Conformalized temporal convolutional quantile regression networks for wind power interval forecasting. *Energy*, 248, 123497.

[28] IEA. 2025. Global energy review 2025. Licence: CC BY 4.0. Paris, (2025). <https://www.iea.org/reports/global-energy-review-2025>.

[29] Ivan Katić, Jørgen Højstrup, and Niels Jensen. 1987. A simple model for cluster efficiency. In.

[30] Yuko Kato, David MJ Tax, and Marco Loog. 2023. A review of non-conformity measures for conformal prediction in regression. *Conformal and Probabilistic Prediction with Applications*, 369–383.

[31] Roger Koenker and Gilbert Bassett Jr. 1978. Regression quantiles. *Econometrica: journal of the Econometric Society*, 33–50.

[32] Matthias Lange. 2005. On the uncertainty of wind power predictions—analysis of the forecast accuracy and statistical distribution of errors. *J. Sol. Energy Eng.*, 127, 2, 177–184.

[33] Yonggang Li, Yue Wang, and Binyuan Wu. 2020. Short-term direct probability prediction model of wind power based on improved natural gradient boosting. *Energies*, 13, 18, 4629.

[34] Kanti V Mardia and Peter E Jupp. 2009. *Directional statistics*. John Wiley & Sons.

[35] Llew Mason, Jonathan Baxter, Peter Bartlett, and Marcus Frean. 1999. Boosting algorithms as gradient descent. *Advances in neural information processing systems*, 12.

[36] James E Matheson and Robert L Winkler. 1976. Scoring rules for continuous probability distributions. *Management science*, 22, 10, 1087–1096.

[37] Amin Niayifar and Fernando Porté-Agel. 2015. A new analytical model for wind farm power prediction. In *Journal of physics: conference series* number 1. Vol. 625. IOP Publishing, 012039.

[38] Jakub Nowotarski and Rafal Weron. 2018. Recent advances in electricity price forecasting: a review of probabilistic forecasting. *Renewable and Sustainable Energy Reviews*, 81, 1548–1568.

[39] European Network of Transmission System Operators for Electricity. 2024. ENTSO-E transparency platform. <https://transparency.entsoe.eu/>. (2024).

[40] Mads M. Pedersen. 2023. Pywake 2.5.0: an open-source wind farm simulation tool, (Feb. 2023). <https://gitlab.windenergy.dtu.dk/TOPFA/RM/PyWake>.

[41] Pierre Pinson. 2013. Wind energy: forecasting challenges for its operational management. *Statistical Science*, 28, 4, 564–585.

[42] Pierre Pinson, Christophe Chevallier, and George N Kariniotakis. 2007. Trading wind generation from short-term probabilistic forecasts of wind power. *IEEE transactions on Power Systems*, 22, 3, 1148–1156.

[43] Yaniv Romano, Evan Patterson, and Emmanuel Candès. 2019. Conformalized quantile regression. *Advances in neural information processing systems*, 32.

[44] Robin Rombach, Andreas Blattmann, Dominik Lorenz, Patrick Esser, and Björn Ommer. 2022. High-resolution image synthesis with latent diffusion models. In *Proceedings of the IEEE/CVF conference on computer vision and pattern recognition*, 10684–10695.

[45] Elia Transmission Belgium SA/NV. 2025. Elia open data platform. <https://opendata.elia.be/>. (2025).

[46] Yves-Marie Saint-Drenan et al. 2020. A parametric model for wind turbine power curves incorporating environmental conditions. *Renewable Energy*, 157, 754–768.

[47] Antonio Segalini and Jan-Åke Dahlberg. 2020. Blockage effects in wind farms. *Wind Energy*, 23, 2, 120–128.

[48] Geert Smet, Joris Van den Bergh, and Piet Termonia. 2023. Probabilistic storm forecasts for wind farms in the north sea.

[49] Yang Song, Jascha Sohl-Dickstein, Diederik P Kingma, Abhishek Kumar, Stefano Ermon, and Ben Poole. 2021. Score-based generative modeling through stochastic differential equations. In *International Conference on Learning Representations*. <https://openreview.net/forum?id=PxTIG12RHS>.

[50] Olivier Sprangers, Sebastian Schelter, and Maarten de Rijke. 2021. Probabilistic gradient boosting machines for large-scale probabilistic regression. In *Proceedings of the 27th ACM SIGKDD conference on knowledge discovery & data mining*, 1510–1520.

[51] Andrea Steiner, Carmen Köhler, Isabel Metzinger, Axel Braun, Matthias Zirkelbach, Dominique Ernst, Peter Tran, and Bodo Ritter. 2017. Critical weather situations for renewable energies—part a: cyclone detection for wind power. *Renewable Energy*, 101, 41–50.

[52] Conor Sweeney, Ricardo J Bessa, Jethro Bowell, and Pierre Pinson. 2020. The future of forecasting for renewable energy. *Wiley Interdisciplinary Reviews: Energy and Environment*, 9, 2, e365.

[53] Diederik van Binsbergen, Pieter-Jan Daems, Timothy Verstraeten, Amir R. Nejad, and Jan Helsen. 2024. Hyperparameter tuning framework for calibrating analytical wake models using scada data of an offshore wind farm. *Wind Energy Science*, 9, 7, (July 2024), 1507–1526. doi:[10.5194/wes-9-1507-2024](https://doi.org/10.5194/wes-9-1507-2024).

[54] Diederik Van Binsbergen, Pieter-Jan Daems, Timothy Verstraeten, Amir Nejad, and Jan Helsen. 2024. Performance comparison of analytical wake models calibrated on a large offshore wind cluster. In *Journal of Physics: Conference Series* number 9. Vol. 2767. IOP Publishing, 092059.

[55] Wei Wang, Bin Feng, Gang Huang, Chuangxin Guo, Wenlong Liao, and Zhe Chen. 2023. Conformal asymmetric multi-quantile generative transformer for day-ahead wind power interval prediction. *Applied Energy*, 333, 120634.

[56] Paige Weber and Matt Woerman. 2024. Intermittency or uncertainty? impacts of renewable energy in electricity markets. *Journal of the Association of Environmental and Resource Economists*, 11, 6, 1351–1385.

[57] 2019. Wind energy generation systems — part 1: design requirements. International Standard. (Feb. 8, 2019). Retrieved May 6, 2025 from <https://webstore.iec.ch/publication/26423>.

[58] Siyi Zhang, Mingbo Liu, Min Xie, and Shunjiang Lin. 2024. Two-stage short-term wind power probabilistic prediction using natural gradient

boosting combined with neural network. *Applied Soft Computing*, 159, 111669.

[59] Xinxin Zhu and Marc G Genton. 2012. Short-term wind speed forecasting for power system operations. *International Statistical Review*, 80, 1, 2–23.

APPENDIX

The set of hyperparameters selected for model tuning is presented in Table IV. It should be noted that the natural gradient boosting model¹ and the conformalized quantile regression model are implemented using XGBoost, whereas the Treeffuser model is based on LightGBM. Consequently, these models require a different set of hyperparameters to tune.

TABLE IV: Tuning parameters for the forecasting models. The continuous uniform distribution between a and b is denoted by $\mathcal{U}(a, b)$ and the log-uniform distribution by $\log \mathcal{U}(a, b)$. We use $\mathcal{U}_D(a, b)$ to denote the discrete uniform distribution.

(a) NGBoost & CQR (XGBoost)

parameter	values
eta	$\mathcal{U}(0.01, 0.2)$
max_depth	$\mathcal{U}_D(3, 7)$
min_child_weight	1, 5, 10, 20
gamma	$\mathcal{U}(0, 1)$
subsample	$\mathcal{U}(0.5, 1)$

(b) Treeffuser (LightGBM)

parameter	values
n_estimators	$\mathcal{U}_D(100, 3000)$
n_repeats	$\mathcal{U}_D(10, 50)$
learning_rate	$\log \mathcal{U}(0.01, 1)$
early_stopping_rounds	$\mathcal{U}_D(10, 100)$
num_leaves	$\mathcal{U}_D(10, 100)$

¹We utilize the natural gradient boosting implementation from the xgb-distribution package, as it has been shown to achieve superior computational efficiency compared to the ngboost library.